Polybaric melting of a single mantle source during the Neogene Siverek phase of the Karacadağ Volcanic Complex, SE Turkey

Taner Ekici[1*], Colin G. Macpherson[2], Nazmi Otlu[1]

[1] Department of Geological Engineering, University of Cumhuriyet, 58140, Sivas, TURKEY

[2] Department of Earth Sciences, University of Durham, Durham, DH1 3LE, UK

* Correspondence author:
tanere7@gmail.com
Tel: +903462191010/1928
Fax: +902191171

Revised version sent to *Lithos,* 1 May 2012

ABSTRACT

Siverek plateau basalts represent the Neogene activity of the Karacadağ Volcanic Complex in southeast Turkey and can be divided into two groups based on incompatible element concentrations. Group 1 is largely basaltic, containing some alkali basalts, while Group 2 consists of alkali basalts, trachybasalts and tephrites. The lavas display a range in major element concentrations that are consistent with restricted amounts of differentiation in the crust. Melts from both groups have experienced variable, small amounts of interaction with crustal rocks, which is responsible for most of the isotopic heterogeneity and caused significant Ba-enrichment. Neither fractional crystallisation nor crustal contamination can account for the differences in trace element enrichment observed between the two groups. Group 1 are derived mainly from the spinel lherzolite field by >1% partial melting. Group 2 lavas were derived from very similar mantle but by smaller degrees of melting and contain a larger relative contribution from garnet-lherzolite. The Siverek plateau lavas are indistinguishable from contemporaneous magmatism in the Karasu Valley of southern Turkey and in northernmost Syria. Together, these plateau basalt fields represent mantle upwelling and melting beneath the thinned and/or weakened Arabian Plate as is migrated northwards during the Neogene.

Keywords: Karacadağ Volcanic Complex, plateau basalt, southern Turkey, intraplate, Arabian Plate

1. Introduction

The Arabian Plate hosts several intraplate basaltic fields and so provides a valuable natural laboratory to explore how this style of magmatism occurs (Camp and Robool 1992; Ilani et al., 2001; Shaw et al., 2003; Krientiz et al., 2006, 2007 and 2009; Ma et al., 2011). The Karacadağ Volcanic Complex in southeast Turkey, sometimes referred to as Karacalıdağ, is one of a number of such fields distributed along the northern edge of the Arabian Plate, where it is in collision with the Anatolian and Eurasian plates (Allen et al., 2004). Until recently, magmatism from this complex was reported to be, exclusively, very young (Pearce et al., 1990; Sen et al., 2004). Petrogenetic models for Karacadağ, and other intraplate fields in northernmost Arabia, have tended to concentrate on the proximity of the Arabian – Anatolian collision in seeking a geodynamic context for melting (e.g. Keskin, 2003; Krientiz et al., 2006). New geochronological data indicate that the Siverek plateau lavas, which constitute the earliest Karacadağ Volcanic Complex activity, extend back into the Middle Miocene, at least (Ekici et al., submitted).

Plateau basalt fields elsewhere in southern Turkey, such as Gaziantep, Kilis and Karacadağ (Gürsoy et al., 2009), in northern Syria (Krienitz et al., 2006), in the Syrian Dead Sea Fault (Ma et al., 2011) and in the Harrat Ash Shaam (Shaw et al., 2003; Krientiz et al., 2007) show two modes in measured ages; earlier magmatism from 30 to 16 Ma and/or 13 to 8 Ma, and then a significant increase in activity since the Pliocene (Ilani et al., 2001). Most of this activity occurred close and parallel to, although not always within, tectonic structures such as the Dead Sea Fault Zone, Euphrates Graben, Sirhan Graben, Karak Graben and Esdraelon Valley (Fig. 1a). Some of these structures, such as the Euphrates Graben, were not tectonically active during magmatism. Therefore, it is important to explore the sources contributing to this type of magmatism and to determine what other factors might cause its association with such structures. In this contribution we focus on the

Siverek lavas of the Karacadağ Volcanic Complex to understand interaction with the crust and the mantle sources of the early activity and to examine relationships to contemporaneous intraplate magmatism elsewhere in Arabia.

2. Geological Setting

The Karacadağ Volcanic Complex, in southeast Turkey, lies immediately south of the Arabian – Anatolian Collision Zone (Fig. 1). The collision is the result of northward motion of the Arabian Plate, with respect to Eurasia and the Anatolian Plate. During the Palaeocene this caused subduction of Neo-Tethyan oceanic lithosphere beneath Anatolia, which terminated with collision and the formation of the Bitlis Suture (Fig. 1a). Continued convergence between Arabia and Eurasia led to westward extrusion of the Anatolian Plate along the Northern- and Eastern Anatolian faults during the Late Miocene (Şengör et al., 2008).

The Karacadağ Volcanic Complex is known to have produced Late Miocene to Quaternary products, possibly with a lithospheric source (Pearce et al., 1990; Ercan et al., 1990; Adiyaman and Chorowicz, 2002; Keskin, 2003; Sen et al., 2004; Brigland et al., 2007; Demir et al., 2007; Lustrino et al., 2010). Ercan et al., (1990) identified three distinct phases; (1) Siverek plateau basalts, (2) alkali basaltic and basanitic lavas flows at Mt. Karacadağ, and (3) young alkali basalts at Ovabağ. New Ar-Ar geochronology confirms the existence of Late Miocene lavas at Siverek but extends the range back to the Middle, and possibly Early, Miocene (Ekici et al., submitted). The Siverek lavas were erupted from ENE-WSW fissure systems at the northern edge of the Karacadağ Volcanic Complex and flowed south. These eruption sites lie south of, but sub-parallel to, the trace of the Bitlis Suture and along the trace of the axis of the Lice Basin (Fig. 1b; Karig and Kozlu, 1990). They are flat-lying plateau basalts, suggesting negligible post eruption deformation at this site.

3. Analytical Methods

Twenty seven samples were analysed for major and trace element concentrations at ACME laboratories (Canada; Table 1). Major element analyses were conducted by X-ray fluorescence upon fused discs prepared by using six parts of lithium tetraborate and one part of rock powder. The mixture was fused in crucibles of 95% Pt and 5% Au at 1050°C for 60 minutes to form a homogeneous melt that was cast into a thick glass disc. Trace element concentrations were analysed by ICP-MS using a fusion method with precision better than ±3% (Online Appendix 2).

Pb, Sr, and Nd isotopes were measured on splits separated from the same 0.2 g aliquots at the University of Geneva using a 7-collector Finnigan MAT 262 thermal ionisation mass spectrometer during December 2008. Samples were processed using procedures described in Chiaradia et al. (2011). The 90° magnetic sector mass analyser has an extended geometry with stigmatic focusing. $^{87}Sr/^{86}Sr$ and $^{143}Nd/^{144}Nd$ ratios were measured in semi-dynamic mode, using double Re filaments. Pb isotopic ratios were obtained in dynamic mode with a single Re filament. $^{88}Sr/^{86}Sr = 8.375209$ was used to correct the mass fractionation of $^{87}Sr/^{86}Sr$, which was compared to the NIST-SRM987 $^{87}Sr/^{86}Sr$ value of 0.710240 ($^{87}Sr/^{86}Sr_{mesured}$ = 0.710240 ± 0.000012 (2 S.E.), n = 31). $^{143}Nd/^{144}Nd$ was mass fractionation corrected relative to a $^{146}Nd/^{144}Nd = 0.721903$ and normalized to the Nd La Jolla standard value of 0.511835 ($^{143}Nd/^{144}Nd_{mesured}$ = 0.511845 ± 0.000004 (2 S.E.), n = 26). Pb isotope data were corrected for instrumental mass fractionation and machine bias by applying a discrimination factor determined by multiple analyses of NBS SRM981, using the reference value of Todt et al. (1984). The discrimination factor averaged 0.00082 +/- 0.00005 (2SE, n=132) per mass unit. These standard analyses were performed over a 6-month period during which the Siverek basalts were analysed. Pb, Sr and Nd blanks were all below their respective detection limits.

4. Results

Precise locations from which samples were collected are provided in Online Appendix 1.

4.1 Petrography

Siverek lavas are olivine-, plagioclase- and augite-phyric basalts, trachybasalts and tephrites with high MgO contents and are dominantly alkaline in character. Generally, they are fresh with little visible sign of alteration other than the presence of minor iddingsite in some olivine crystals. Loss on ignition values are generally low with only a small number in excess of 2 wt.% and all less than 3 wt.% (Table 1). Siverek lavas are fine-grained and contain less than 25 modal % phenocrysts. Olivine and plagioclase are ubiquitous and are the most abundant phenocrysts with smaller quantities of clinopyroxene present in many lavas. No xenoliths or xenocrysts were identified either in hand sample or during microscopic examination.

4.2 Major and trace elements

Silica contents of Siverek lavas range from 43.57 to 49.63 wt.% while MgO contents vary between 12.12 and 3.97 wt.%. Based on their major and trace element compositions two groups of Siverek lavas can be recognised (Fig. 2). Compared to Group 1, Group 2 lavas have relatively high concentrations of incompatible elements, notably K_2O, TiO_2, and P_2O_5 and most incompatible trace elements. While there is less distinction between the groups for the compatible elements it is still possible to recognise differences between them. In Group 1 MgO correlates negatively with Al_2O_3. There are weaker, negative correlations of MgO with SiO_2 and CaO, and a positive correlation with Fe_2O_3. Group 2 also shows a strong negative correlation with Al_2O_3 while the remaining major elements display more scatter but are generally displaced to lower SiO_2 than Group 1.

Several incompatible trace elements are relatively invariant in Group 1 lavas (Fig. 3). The high field strength elements, light rare earth elements and Sr show negligible variation across the range of MgO contents. Ba is a notable exception with three lavas being enriched by a factor of two compared to the rest of this group. Rb also shows a significant amount of scatter while the heavy rare earth elements increase with decreasing MgO. Group 2 lavas also show behaviour consistent with that observed for their major elements being displaced to higher concentrations and, although more variable than Group 1, several elements e.g. Sr, Zr and Nb, display restricted variation with MgO in Group 2 samples. Two exceptions to this are DS48 and DS49, which possess significantly higher concentrations of several, but not all, incompatible elements than the rest of Group 2.

Normalised incompatible element diagrams show inter-element ratios to be similar in the two groups (Fig. 4). Group 1 lavas show moderate degrees of enrichment of the most incompatible elements relative to primitive mantle with pronounced negative anomalies in Pb and, to lesser extent P, whilst the heavy rare earth elements and Y are also relatively depleted. Overall, Group 2 lavas show similar patterns but with greater enrichment in all elements except the heavy rare earth elements and Y, which have similar concentrations to Group 1 (Fig. 4). However, the Group 2 lavas do possess even greater enrichment in Rb and Ba than Group 1. Lustrino et al. (2010) did not differentiate two groups in their Siverek Plateau Series but the range of compositions presented are similar to our overall data without showing a clear distinction into either group that we have recognised. Alkali basalt from NW Syria that has escaped crustal contamination (Krienitz et al., 2006) displays very similar trace element ratios to Siverek Group 2 lavas (Fig. 4b), which also resembles patterns for Harrat Ash Shaam (Shaw et al., 2003). The Siverek lavas lack the K-depletion of, and are more P-depleted than, Late Neogene lavas from the Syrian sector of the Dead Sea Fault (Ma et al., 2011).

4.3 Sr-Nd-Pb isotope ratios

Samples representing the range of chemical characteristics of Groups 1 and 2 were chosen for isotopic analysis. Ranges for isotopic ratios in the Siverek lavas are $^{87}Sr/^{86}Sr$; 0.703724 to 0.705651, $^{143}Nd/^{144}Nd$; 0.512836 to 0.512539, $^{206}Pb/^{204}Pb$; 18.830 to 19.016, $^{207}Pb/^{204}Pb$; 15.59 to 15.68; and $^{208}Pb/^{204}Pb$; 38.739 to 39.517 (Table 2). These are wider ranges than those previously observed for most Arabian intra-plate magmatic sites (Shaw et al., 2003; Krienitz et al., 2009; Ma et al., 2011) and previously determined for the Siverek lavas by Lustrino et al. (2010). The lowest $^{87}Sr/^{86}Sr$ and highest $^{143}Nd/^{144}Nd$ ratios, however, are similar to values previously determined for Neogene magmatism at Siverek and for NW Syria (Fig. 5).

5. Discussion

In this section we will evaluate the processes that have modified Siverek magma subsequent to its generation in the mantle, then determine the mantle sources and compare these to other Arabian intraplate magmatic suites.

5.1 Fractional Crystallisation

Several Siverek lavas possess relatively evolved compositions (e.g. MgO < 6wt. %) suggesting that they have experienced some degree of fractional crystallisation. This is consistent with the ubiquitous presence of olivine and plagioclase, and common clinopyroxene, as phenocryst phases in the rocks. However, the relatively restricted range of major element contents in most of the lavas indicate that this process has exerted little influence on the compositions. In particular, the incompatible elements display little absolute variation across the range of MgO and SiO_2 contents. Specifically, incompatible elements that would be expected to increase in concentration during fractional crystallisation of the phenocryst assemblage, such as Nb, Zr and La, show no significant variation across either group (Fig. 3). The lack of Sr enrichment might be attributed to plagioclase crystallisation, although the increase in Al_2O_3 with decreasing MgO would indicate that this is unlikely to be the case (Fig. 2). Fractional crystallisation may have caused relatively small changes in the concentrations of major elements, for example producing some of the most evolved lavas with MgO < 6 wt.%. But we conclude that fractional crystallisation is not responsible for differences in concentrations of most elements between Groups 1 and 2 and has done little to modify most element - element ratios.

5.2 Crustal contamination

Interaction between intraplate magma and Arabian crust has been recognised at several localities through the use of various isotopic and trace element indicators (Baker et al., 2000; Shaw et al., 2003; Krienitz et al., 2009; Ma et al., 2011). No crustal xenoliths have been found in the Siverek plateau lavas. Similarly, microscopic examination has revealed no evidence for crustal fragments or xenocrysts in the rocks. However, the range of Sr, Nd and Pb isotopic ratios determined in this work is greater than that previously proposed for mantle sources beneath several north Arabian intraplate magmatic fields. Lustrino et al. (2010) claimed that interaction between melt and crust should produce correlations between isotopic ratios and SiO_2. They interpreted the absence of such relationships in Siverek lavas as evidence that there had been little crustal contamination. However, this reasoning assumes negligible SiO_2 variation amongst parental magma batches and, so, ignores the potential of different depths and degrees of partial melting to influence initial silica content of basaltic melt (Shaw et al., 2003; Krientiz et al., 2006 and 2009; Ma et al., 2011).

The crust beneath southeast Turkey, and other parts of the northern Arabian Plate, is not well known. This complicates the task of trying to identify the influence of crustal contamination upon the geochemical variation in lavas. Isotopic variation in basaltic rocks from Harrat Ash Shaam and the Northern Dead Sea Fault has previously been attributed to crustal interaction (Shaw et al., 2003; Krienitz et al., 2009; Ma et al., 2011). Therefore, our approach is to try and indentify chemical variation within the Siverek suite that might result from such processes.

Isotopic indicators of crustal contamination are not preferentially associated with Group 1 or 2. Instead, the lowest $^{87}Sr/^{86}Sr$ and highest $^{143}Nd/^{144}Nd$ measured for both Groups 1 and 2 are virtually indistinguishable from the respective equivalents in the dataset of Lustrino et al. (2010). Higher $^{87}Sr/^{86}Sr$ and lower $^{143}Nd/^{144}Nd$ occur in both Group 1 and Group 2 rocks. Thus, if melt – crust interaction is responsible for the isotopic heterogeneity then it has affected both groups and is not responsible for the differences in trace element concentrations between the two groups. A role for crustal contamination is also suggested by Pb isotopic ratios which for any given $^{206}Pb/^{204}Pb$ are displaced to higher $^{207}Pb/^{204}Pb$ ($\Delta 7/4$) and $^{208}Pb/^{204}Pb$ ($\Delta 8/4$) than the Northern Hemisphere Reference Line (Fig. 7). The extent of this displacement, as demonstrated by plots of $\Delta 7/4$ versus $\Delta 8/4$, are similar to that observed for Miocene to Quaternary volcanics from NW Syria and the Karasu Valley in southern Turkey, and slightly greater than that for Harrat Ash Shaam (Fig. 7).

Few trace element ratios in the Siverek volcanics display strong correlations with isotopic ratios, but Ba enrichment is associated with more radiogenic Sr in our dataset (Fig. 6a) and less radiogenic Nd isotopic ratios. Ba contents are also more scattered than those of most other trace elements (Fig. 3). Specifically, high $^{87}Sr/^{86}Sr$ is found in rocks with high Ba/Yb ratios and Ba-enrichment shows far greater scatter than other trace element ratios when plotted against indices of chemical enrichment (Fig. 6b). This Ba-enrichment is unlikely to result from the presence of caliche as identified in some Harrat Ash Shaam lavas (Shaw et al., 2003) because (1) the enrichment of Ba over other incompatible trace elements is not in excess of crustal values, and (2) Ba-rich samples show no concomitant increase in Sr concentrations. Nb/U ratios are displaced to lower values than expected for mantle derived melts and may also indicate addition of a crustal component (Krienitz et al., 2006).

Prior studies of northern Arabian magmatism have attributed contamination to upper crustal materials but have recognised the lack of data for suitable crustal rocks with which to make such comparisons (Shaw et al., 2003; Krienitz et al., 2006 and 2009; Ma et al., 2011). We have chosen to model contamination by upper and lower crustal rocks from northeast Africa (Sudan) because these offer trace element and Sr, Nd and Pb isotopic compositions with which to constrain the role of crust. We emphasise that we are not trying to advocate any shared provenance between Sudanese and Turkish basement but to test the potential of upper versus lower crustal rocks as contaminants within the same lithospheric block from which the Arabian Plate originated.

The models illustrated in Fig. 7a demonstrate that the array of Sr-Nd isotopic ratios at Siverek can be produced by less than 10% differentiation for either a Group 1 or Group 2 initial melt. For an assimilation to crystallisation ratio of c. 0.75 this equates to $<5\%$ addition of contaminant to the initial melts. The Pb isotopic variation in the model requires even less addition of crust (Fig. 7b & c), although the exact amount is highly dependent on the ratio of Pb concentrations in the melt and contaminant, which is very poorly constrained. Such restricted amounts of contamination are likely to have relatively little impact on the major element concentrations in the melts.

It is possible to produce the range of isotopic compositions observed at Siverek with relatively small amounts of contamination by either upper or lower crust (Fig. 7). Successful models can be achieved because of the significant heterogeneity in the contaminant dataset we have chosen but such heterogeneity is likely to be a real feature of any crustal terrane with which melts interact. The isotopic data for most Siverek (and other southern Turkish, Syrian, Lebanese and Jordanian) lavas are consistent with upper or lower crust as the contaminant (Fig. 7a-c). However, the most contaminated Siverek rock (DS-34) has extremely elevated $\Delta 7/4$ and $\Delta 8/4$, which might be interpreted as a lower crustal contaminant (Fig. 7d). Furthermore, the upper crustal rocks have relatively modest enrichment in Ba, relative to other trace elements (Davidson and Wilson, 1989). Notwithstanding the fractionation that might occur during anatexis of crustal rocks, they provide significantly less leverage for Ba enrichment than the lower crustal lithologies from Sudan, which possess Ba/Yb ratios of 4500 - 5200. Thus, while the Sr and Nd isotopic data are readily explained by upper crustal contamination, the Pb isotope ratios and Ba enrichment suggest that lower crustal rocks may also have interacted with the melts.

Isotopic variation in Siverek lavas suggest that crustal Sr, Nd and Pb has been acquired by Siverek magmas during passage through the Arabian lithosphere. Ba enrichment is associated with increased $^{87}Sr/^{86}Sr$ and decreased $^{143}Nd/^{144}Nd$ (Fig. 6) suggesting that this process has also added significant amounts of Ba to the magma. Thus, we conclude that there was a restricted amount of contamination of Siverek magma by upper, and possibly some lower, crust that exerted the principle control on the isotopic variation at Siverek. The coincidence of lowest $^{87}Sr/^{86}Sr$ and highest $^{143}Nd/^{144}Nd$ in our Group 1 and 2 samples with those of Lustrino et al. (2010) lead us to conclude that these values are representative of the mantle beneath the northern-most Arabian plate during the Siverek magmatism. However, with the exception of Ba-enrichment, crustal contamination has had negligible influence upon other major and trace element characteristics of the Siverek lavas.

5.3 Mantle Sources

Constraints from trace elements and isotopic data indicate that magma differentiation and crustal contamination have caused little perturbation of the initial composition of Siverek magma. Thus, variations of incompatible trace element ratios can be used to investigate what was responsible for the range of melt compositions generated in the mantle beneath the northern Arabian Plate during the Neogene.

Siverek lavas display a more restricted range of silica contents that those found in Harrat Ash Shaam or in the northern Dead Sea Fault (Shaw et al., 2003; Krienitz et al., 2009; Ma et al., 2011). This is due to the absence of very silica poor (< 43 wt.%

SiO_2) basanites discovered at those other sites. As such, there is no need to invoke mafic components, such as pyroxenite or hornblendite veins, in the source of Siverek lavas, as has been done for Late Neogene magmatism in and around the Dead Sea Fault (Weinstein et al., 2006; Ma et al., 2011). The lack of pronounced K-depletion at Siverek, where all lavas posses values for $(K/La)_n > 0.73$, and the absence of a negative correlation between SiO_2 and $(Sm/Zr)_n$, for which all values are less than $<$ 0.95, are also consistent with a peridotitic, not a mafic, source. K-depletion is present in some primitive, Middle Miocene lavas from Harrat Ash Shaam (Shaw et al., 2003; Krienitz et al., 2007) suggesting that mafic components may have melted in the Arabian mantle at that time. However, the Siverek plateau basalt field has been intensively sampled (Lustrino et al., 2010; this work) so we regard it as unlikely that low-silica lavas were erupted at Siverek. Therefore, we proceed on the assumption that any mafic reservoir was not involved in petrogenesis of Siverek plateau basalts and that melting was restricted to the peridotitic mantle beneath this part of the Arabian Plate.

Group 1 and Group 2 lavas display clear distinctions in rare earth element fractionation. Fig. 8a compares primitive mantle-normalised La/Yb and Dy/Yb ratios of all Siverek lavas with the results of non-modal fractional melting models for primitive and enriched spinel- and garnet lherzolite. While La/Yb is most sensitive to the degree of partial melting, Dy/Yb responds to the presence or absence garnet in the melt residue and, thus, allows relative contributions from deep and shallow melt fractions to be estimated (Shaw et al., 2003). Group 1 lavas possess a restricted range of low La/Yb and Dy/Yb ratios. For a primitive mantle source, these melts are not consistent with melts derived purely from spinel- or garnet-bearing lherzolite (Fig. 8a). Instead, the Dy/Yb ratios require mixtures derived from both shallow and deep lithologies. The Group 2 lavas extend to significantly higher La/Yb and Dy/Yb values indicating greater contributions from the deeper, garnet lherzolite source. Mixed deep and shallow melts are also consistent with the major element systematic of the

Siverek lavas. Group 1 composition vary between a deep, low-SiO_2 and a shallow, high-SiO_2 endmember (Fig. 2). Fractional crystallisation and crustal contamination can explain some of the scatter in the major element arrays. Group 2 lavas show more scatter which may be as a result of the smaller degrees of partial melting involved.

Fig. 8b plots only those Siverek lavas that we are most confident have escaped any crustal contamination. The criterion was to use only samples with low Ba/Yb relative to other trace element ratios; e.g. those samples with the lowest Ba/Yb for any given La/Yb (Fig. 6b). These samples are compared with a model for melting of peridotite enriched in trace elements as described by Shaw et al. (2003). While the most elevated Dy/Yb ratios for Siverek lavas do not require an enriched mantle source they do plot close to the Harrat Ash Shaam data, suggesting similar degrees of melting of similar sources. The Group 1 and Group 2 lavas still fall between the spinel- and garnet-lherzoilte melting curves but the Group 1 lavas are now consistent with derivation almost exclusively from the lower-pressure source. The Group 1 lavas are displaced to lower La/Yb than Group 2 indicating greater degrees of partial melting, which is consistent with the concentrations of incompatible elements in the two groups. The same conclusion is reached when the unfiltered Siverek dataset is considered (Fig. 8a) re-enforcing our contention that crustal contamination has had a negligible influence on most incompatible trace element ratios. The degrees of partial melting inferred for Group 1 are similar to those estimated from Harrat Ash Shaam (Fig. 8b) while Group 2 indicate lower degrees of partial melting.

Siverek lavas are mixtures of melts derived from spinel- and garnet-peridotite. Group 1 lavas were produced by higher degrees of partial melting than those of Group 2. Both groups were derived by melting over a range of depths, the lower degree melts of Group 2 containing more significant input from deeper mantle. We detect no isotopic distinction between Group 1 and 2 for Sr and Nd isotopic ratios. The data indicate some variation in initial Pb isotopic compositions, as previously observed for

Syrian and Jordanian magmatism (Shaw et al., 2003; Krienitz et al., 2009; Ma et al., 2011). This probably reflects long-term heterogeneity in U/Th ratios of the source. The majority of variation in Δ7/4 and Δ8/4 at Siverek, and probably other Turkish and Syrian localities, reflects crustal contamination (Fig. 7). The low Δ8/4 relative to Δ7/4 of the least contaminated Siverek lavas indicate that this source is distinct from that of magmatism attributed to the Afar plume. This trait is shared by the vast bulk of Neogene to recent magmatism in southern Turkey, Syria, Jordan and Lebanon, with only a couple of exceptions from the Northern Dead Sea Fault in Syria (Fig. 7d). Therefore, we conclude that there has been negligible involvement of mantle derived from the Afar region in northern Arabia.

5.4 Mantle Melting

Previous attempts to understand the origin of the Karacadağ Volcanic Complex and magmatism elsewhere in the northernmost Arabian plate have generally focussed on the proximity of this site to the Arabian – Anatolian plate boundary. Mechanisms have been sought that advocate geodynamic forces generated by the collision between these plate and/or deformation of the subducted Neo-Tethyan lithosphere that formerly separated them (Keskin, 2003; Krienitz et al., 2006 and 2009). Some studies have also proposed a role for mantle derived from the Afar plume (Camp and Roobol, 1992; Ilani et al., 2001; Krientiz et al., 2009). As demonstrated above, the Pb isotope composition of northern Arabian magmatism is not consistent with a contribution from Afar.

In the absence of evidence for anomalously hot mantle derived from Afar, or of lithosphere-hosted enrichments, such as mafic veins (Ma et al., 2011), Siverek magmatism must be the product of upwelling of asthenospheric mantle. Extension is the most commonly proposed mechanism for facilitating mantle upwelling and has been advocated for intraplate magmatism in some parts of the Arabian Plate (Shaw et al., 2003; Tatar et al., 2004). However, Krienitz et al. (2006) claim that there was insufficient lithospheric stretching across the Sirhan Graben, or other sites of Arabian intraplate magmatism e.g. Euphrates Graben, to cause basaltic petrogenesis by extension alone. Furthermore, the ENE - WSW fissure system from which Siverek lavas were erupted is not consistent with tension resulting from the north-easterly to northward motion of the Arabian plate since the Oligocene (McQuarrie et al., 2003).

King and Anderson (1988) proposed that upwelling adjacent to continental edges may drive melting. Siverek magmas were erupted towards the northern edge of the northward migrating Arabian plate while the oceanic lithosphere to the north was being subducted. If the margin thinned significantly towards the adjacent oceanic lithosphere to the north then this could have been a location for density driven upwelling at a continental edge. Alternatively, Conrad et al. (2011) propose that intraplate magmatism around the globe over the last 10 million years has occurred at sites of high asthenospheric shear. This could reflect melting as mantle upwells into thinspots or low viscosity cavities at the base of the lithosphere (Conrad et al., 2010). Such upwelling will occur wherever cavities exist, regardless of whether the lithosphere is deforming at that time. Thus, melting might occur beneath thinspots or weakspots that are inactive, or at least not stretching enough to generate magmatism through extension alone (Macpherson et al., 2010). Furthermore, magmatism will reflect upwelling into relief at the base of the mantle, which may not be exactly vertically contiguous with surface expressions of lithospheric weakness or deformation. Surface structures, active or otherwise, associated with relief on the lithospheric base will have the potential to influence local distribution of volcanism at the surface but will not always be exactly coincident with it.

Prior to collision, the Arabian Plate would have thinned towards the Neo-Tethyan oceanic crust that was subducted beneath Anatolia. Deformation of the northern plate margin would have occurred due to (i) forces generated within the Arabian Plate by the collision, (ii) tension exerted on the continent margin by the ongoing subduction of the Neo-Tethyan slab, and (iii) resistance of the Anatolian Plate. Thus, the lithosphere beneath southern Turkey is likely to display physical and rheological contrast with the lithosphere to both north and south. The forces generated during the collision are thought to be responsible for formation of the Lice Basin, which has been interpreted as either a flexural response of the Arabian Plate to loading by the Bitlis Massif or as a transtensional feature produced by the collision (Karig and Kozlu, 1990; Robertson, 2000). There was little stretching perpendicular to the length of this feature but Early Miocene sedimentation and tectonism records significant lithospheric deformation as the collision between Arabian and Anatolian plates culminated. Siverek magmatism was erupted from ENE-WSW striking fissures that are sub-parallel to the fabric produced by the Arabian – Anatolian collision and that lie close to the axis of the Lice Basin. Therefore, we interpret the Siverek phase of the Karacadağ Volcanic Complex as melting that occurred below Arabian lithosphere that was inherently thin and was possibly further weakened as a result of the collision with the Anatolian Plate. Northward migration of the Arabian Plate allowed the mantle to upwell and melt where the Plate was thin and/or weak(Conrad et al., 2011).

6. Conclusions

Siverek plateau basalts were derived solely from peridotitic mantle, with no contribution from mafic (hornblendite or amphibole-garnet-pyroxenite) veins in the lithospheric mantle. The two groups with different trace element concentrations were derived from isotopically similar sources and their distinction can be explained by different degrees of partial melting across a range of depths. Group 1 lavas are dominated by melt produced from spinel-lherzolite, while Group 2 are smaller degree partial melts of the same mantle containing a greater relative contribution from garnet-lherzolite. We find no evidence for isotopic heterogeneity between deep and shallow sources, as proposed for Harrat Ash Shaam (Shaw et al., 2011) or for melting of mafic enrichments in the lithospheric mantle (Ma et al., 2011). Mantle derived from the Afar Triple Junction was not involved in genesis of the Siverek lavas. Instead, mantle upwelled as the thin, and possibly weakened, lithosphere of the northern Arabian margin migrated northwards.

Acknowledgements

Taner Ekici acknowledges financial support from TUBITAK (Project No. 107Y025) to conduct fieldwork and analytical work. Mehmet Ülkü of MTA Diyarbakır supported fieldwork in SE Turkey. Discussion with Gillian Foulger was valuable in refining a number of concepts discussed. Kurt Knesel and an anonymous reviewer provided very constructive and helpful reviews. Colin Macpherson is grateful to Durham University for a period of research leave.

References

Adıyaman, Ö., Chorowicz, J., 2002. Late Cenozoic tectonics and volcanism in the northwestern corner of the Arabian plate: a consequence of the strike-slip Dead Sea fault zone and the lateral escape of Anatolia. Journal of Volcanology and Geothermal Research 117, 327-345.

Allen, M., Jackson, J., Walker, R., 2004. Late Cenozoic reorganization of the Arabia-Eurasia collision and the comparison of short-term and long term deformation rates. Tectonics 23, TC2008, doi: 10.1029/2003TC001530.

Baker, J.A., Macpherson, C.G., Menzies, M.A., Thirlwall, M.F., Al-Kadasi, M., Mattey, D.P., 2000. Resolving crustal and mantle contributions to continental flood volcanism, Yemen: Constraints from mineral oxygen isotope data. Journal of Petrology 41, 1805-1820.

Brigland, D., Demir, T., Seyrek, A., Pringle, M., Westaway, R., Beck, A., Yurtmen, S., Rowbotham, G., 2007. Dating Quaternary volcanism and incision by the River Tigris at Diyarbakır, SE Turkey. Journal of Quaternary Science 21, 437-455, doi: 10.1002/jqs.1074.

Camp, V.E., Roobol, M.J., 1992. Upwelling Asthenosphere beneath western Arabia and its regional implications. Journal of Geophysical Research 97, 15,255-271.

Chiaradia, M., Müntener, O., Beate, B., 2011. Enriched basaltic andesites from mid-crustal fractional crystallization, recharge, and assimilation (Pilavo volcano, Western Cordillera of Ecuador). Journal of Petrology 52, 1107-1141, doi: 10.1093/petrology/egr020.

Conrad, C.P., Wu, B., Smith, E.I., Bianco, T.A., Tibbetts, A., 2010. Shear-driven upwelling induced by lateral viscosity variations and asthenospheric shear: A mechanism for intraplate volcanism. Physics of the Earth Planetary Interiors 178, 162-175. doi:10.1016/j.pepi.2009.10.001.

Conrad, C.P., Bianco, T.A., Smith, E.I., Wessel, P., 2011. Patterns of intraplate volcanism controlled by asthenospheric shear. Nature Geoscience 4, 317-321, doi:10.1038/NGEO1111.

Çapan, U.Z., Vidal, P., Contagrel, L.M., 1987. K-Ar, Nd, Sr and Pb isotopic study of Quaternary volcanism in Karasu Valley (Hatay), N end of Dead Sea rift zone in SE Turkey. Yerbilimleri 14, 165-178.

Davidson, J.P., Wilson, I.R., 1989. Evolution of an alkali basalt-trachyte suite from Jebel Marra volcano, Sudan, through assimilation and fractional crystallisation. Earth and Planetary Science Letters 95, 141-160.

Demir, T., Westaway, R., Brigland, D., Pringle, M., Yurtmen, S., Beck, A., Rowbotham, G., 2007. Ar-Ar dating of late Cenozoic basaltic volcanism in northern Syria: Implications for the history of incision by the River Euphrates and uplift of the northern Arabian Platform. Tectonics 26, TC3012, doi:10.1029/2006TC001959.

Deniel, C., Vidal, P., Coulon, C., Vellutini, P.J., Piquet, P., 1994. Temporal evolution of mantle sources during continental rifting: the volcanism of Djibouti (Afar). Journal of Geophysical Research 99, 2853-2869.

Ekici, T., Macpherson, C.G. & Otlu, N. (2011). Intraplate magmatism generated by shear-induced melting during Arabian plate motion: Evidence from Karacadağ Volcanic Complex, southeast Turkey. Submitted to *Journal of the Geological Society of London*.

Ercan, T., Fujitani, T., Matsuda, J.I., Notsu, K., Tokel, S., ve Ul, T., 1990. Doğu ve Güneydoğu Anadolu Neojen-Kuvaterner Volkanitlerine ilişkin yeni jeokimyasal, radyometrik ve izotopik verilerin yorumu. MTA Dergisi 110, 143-164.

Gürsoy, H., Tatar, O., Piper, J.D.A., Koçbulut, F., Mesci, B.L., 2009. Paleomagnetic study of Tertiary volcanic domains in Southern Turkey and Neogene anticlockwise rotation of the Arabian Plate. Tectonophysics 465, 114-127, doi:10.1016/j.tecto.2008.11.001.

Hart, S.R., 1984. A large-scale isotope anomaly in the Southern Hemisphere mantle. Nature 309, 753-757.

Hempton, M.R., 1987. Constraints on Arabian plate motion and extensional history. Tectonics 6, 687-705.

Ilani, S., Harlavan, Y., Tarawneh , K., Rabba, I., Weinberger, R., Ibrahim, K., Peltz, S., Steinitz, G., 2001. New K-Ar ages of basalts from the Harrat Ash Shaam volcanic field in Jordan: Implications for the span and duration of the upper-mantle upwelling beneath the western Arabian plate. Geology 29, 171-174.

Karig, D.E., Kozlu, H., 1990. Late Palaeogene-Neogene evolution of the triple junction region near Maraş, south-central Turkey. Journal of the Geological Society 147, 1023-1034, doi: 10.1144/gsjgs.147.6.1023.

Keskin, M., 2003. Magma generation by slab steepening and breakoff beneath a subduction-accretion complex: An alternative model for collision-related volcanism in Eastern Anatolia, Turkey. Geophysical Research Letters 30, 8046, doi:10, 1029/2003GL018019.

King, S.D., Anderson, D.L., 1998. Edge-driven convection. Earth and Planetary Science Letters 160, 289-296.

Krienitz, M.S., Haase, K.M., Mezger, K., Eckardt, V., Shaikh-Mashail, M.A., 2006. Magma genesis and crustal contamination of continental intraplate lavas in Northwestern Syria. Contributions to Mineralogy and Petrology 151, 698-716, doi10.1007/s00410-006-0088-1.

Krienitz, M.S., Haase, K.M., Mezger, K., Shaikh-Mashail, M.A., 2007. Magma genesis and mantle dynamics at Harrat Ash Shamah volcanic field (Southern Syria). Journal of Petrology 48, 1513-1542, doi:10.1093/petrology/egm028.

Krienitz, M.S., Haase, K.M., Mezger, K., Van den Bogard, P., Thiemann, V., Shaikh-Mashail, M.A., 2009. Tectonics events, continental intraplate volcanism, and mantle plume activity in northern Arabia: Constraints from geochemistry and Ar-Ar dating of Syrian lavas. Geochemistry Geophysics Geosystems 10, Q04008, doi:10.1029/2008GC002254.

Lustrino, M., Keskin, M., Mattioli, M., Lebedev, V.A., Chugaev, A., Sharkov, E., Kavak, O., 2010. Early activity of the largest Cenozoic shield volcano in the circum-Mediterranean area: Mt. Karacadağ, SE Turkey. European Journal of Mineralogy 22, 343-362, doi:10.1127/0935-1221/2010/0022-2024.

Ma, G.S.-K., Malpas, J., Xenophontos, C., Chan, G.H.-N., 2011. Petrogenesis of latest Miocene-Quaternary continental intraplate volcanism along the northern Dead Sea Fault system (Al Ghab – Homs volcanic field), western Syria: Evidence for lithosphere – asthenosphere interaction. Journal of Petrology 52, 401-430, doi:10.1093/petrology/egq085.

Macpherson, C.G., Chiang, K.K., Hall, R., Nowell, G.M., Castillo, P.R., Thirlwall, M.F., 2010. Plio-Pleistocene intra-plate magmatism from the southern Sulu Arc, Semporna peninsula, Sabah, Borneo: Implications for high-Nb basalt in subduction zones. Journal of Volcanology and Geothermal Research 190, 25-38. doi:10.1016/j.jvolgeores.2009.11.004.

Marschik, R., Fontignie, D., Chiarardia, M., Voldet, P., 2003. Geochemical and Sr-Nd-Pb-O isotope composition of granitoids of the Early Cretaceous Copiapó plutonic complex (27°30'S), Chile. Journal of South American Earth Sciences 16, 381-398, doi:10.1016/S0895-9811(03)00104-4.

McDonough, W.F., Sun, S.S., 1995. The composition of the Earth. Chemical Geology 120, p. 223-253.

McKenzie, D. & O'Nions, R.K. (1991). Partial melt distributions from inversion of rare earth element concentrations. *Journal of Petrology* **32**, 1021-1091.

McQuarrie, N., Stock, J.C., Verdel, C., Wernicke, B.P., 2003. Cenozoic evolution of Neotethys and implications for the causes of plate motions. Geophysical Research Letters 30, 20,2036. doi:10.1029/2003GL017992.

Pearce, J.A., Bender, J.F., DeLong, S.E., Kidd, W.S.F., Low, P.J., Güner, Y., Şaroğlu, F., Yılmaz, Y., Moorbath, S., Mitchell, J.G., 1990. Genesis of collision volcanism in eastern Anatolia, Turkey. Journal of Volcanology and Geothermal Research 44, 184-229.

Pik, R., Deniel, C., Coulon., Yirgu, G., Marty, B., 1999. Isotopic and trace element signatures of Ethiopian flood basalts: evidence for plume-lithosphere interactions from Na/Ti and rare earth element ratios. Journal of Geophysical Research 104, 2817-2829.

Robertson, A.H.F., 2000. Mesozoic-Tertiary tectonic-sedimentary evolution of a south Tethyan oceanic basin and its margins in southern Turkey In: Bozkurt, E., Winchester, J.A., Piper, J.D.A. (Eds.), Tectonics and Magmatism in Turkey and the Surrounding Area. Geological Society of London Special Publications 173, 97-138.

Shaw, J.E., Baker, J.A., Menzies, M.A., Thirlwall, M.F., Ibrahim, K.M., 2003. Petrogenesis of the largest intraplate volcanic field on the Arabian Plate (Jordan): a mixed Lithosphere-Asthenosphere source activated by Lithospheric extension. Journal of Petrology 44, 1657-1679, doi:10.1093/petrology/egg052.

Şen, P.A., Temel, A., Gourgaud, A., 2004. Petrogenetic modelling of Quaternary post-collisional volcanism: A case study of central and eastern Anatolia. Geological Magazine 141, 81-98, doi: 10.1017/S0016756803008550.

Şengör, A.M.C., Özeren, M.S., Keskin, M., Sakınç, M., Özbakır, A.D., Kayan, İ., 2008. Eastern Turkish high plateau as a small Turkish-type orogen: Implications for post-collisional crust forming processes in Turkish-type orogens. Earth Science Reviews 90, 1-48, doi:10.1016/j.earscirev.2008.05.002.

Tatar, O., Piper, J.D.A., Gürsoy, H., Heimann., Koçbulut, F., 2004. Neotectonic deformation in the transition zone between the Dead Sea Transform and the east Anatolian fault Zone, Southern Turkey: a palaeomagnetic study of the Karasu Rift Volcanism. Tectonophysics 385, 17-43. doi:10.1016/j.tecto.2004.04.005.

Thirlwall, .F., Upton, B.G.J., Jenkins, C., 1994. Interaction between continental lithosphere and the Iceland plume – Sr-Nd-Pb isotope geochemistry of Tertiary basalts, NE Greenland. Journal of Petrology 35, 839-879.

Todt, W., Cliff, R.A., Hanser, A., Hoffmann, A.W., 1984. ^{202}Pb+^{205}Pb double spike for lead isotopic analyses. Terra Cognita 4, 209.

Weinstein, Y., Navon, O., Altherr, R., Stein, M., 2006. The role of lithospheric mantle heterogeneity in the generation of Plio-Pleistocene alkali basaltic suites from NW Harrat Ash Shaam (Israel). Journal of Petrology 47, 1017-1050.

Figure Captions

Figure 1. (a) Map of Northern Arabia showing the location of Neogene to Recent volcanic fields and major tectonic elements. (b) Map of southeast Turkey showing the location of the Siverek volcanic within the Karacadağ Volcanic Complex. Maps modified from Ilani et al (2001), Gürsoy et al. (2009) and Krienitz et al. (2009).

Figure 2. Plots of selected major elements versus MgO for Siverek lavas from Karacadağ Volcanic Complex. Data from Lustrino et al (2010) included for comparison.

Figure 3. Plots of selected trace elements versus MgO for Siverek lavas from Karacadağ Volcanic Complex. Data from Lustrino et al (2010) included for comparison.

Figure 4. Incompatible trace element concentrations of lavas normalised to primitive mantle (McDonough and Sun, 1995). (a) Range of values for Siverek Group 1 lavas. (b) Range of values for Siverek Group 2 and NW Syrian alkali basalt with minimal crustal contamination (Krientiz et al., 2006). (c) Siverek plateau stage lavas from Lustrino et al. (2010).

Figure 5. (a) $^{87}Sr/^{86}Sr$ versus $^{143}Nd/^{144}Nd$, (b) $^{206}Pb/^{204}Pb$ versus $^{207}Pb/^{204}Pb$, and (c) $^{206}Pb/^{204}Pb$ versus $^{208}Pb/^{204}Pb$ for lavas from the Siverek phase of the Karacadağ Volcanic Complex. Previously published data for Siverek lavas from Lustrino et al

(2010) included for comparison with data from Karasu Valley (Çapan et al., 1987) and NW Syria (Krienitz et al., 2006).

Figure 6. (a) Ba/Yb versus $^{87}Sr/^{86}Sr$, (b) Ba/Yb versus La/Yb for lavas from the Siverek phase of the Karacadağ Volcanic Complex. Data from Lustrino et al (2010) included for comparison.

Figure 7. (a) $^{87}Sr/^{86}Sr$ versus $^{143}Nd/^{144}Nd$, (b) $^{206}Pb/^{204}Pb$ versus $^{207}Pb/^{204}Pb$, and (c) $^{206}Pb/^{204}Pb$ versus $^{208}Pb/^{204}Pb$ for Siverek lavas. Previously published data for Siverek lavas from Lustrino et al (2010) included for comparison with data from Karasu Valley (Çapan et al., 1987), NW Syria (Krienitz et al., 2006), the Northern Dead Sea Fault (Ma et al., 2011), Harrat Ash Shaam (Shaw et al., 2003) and lavas attributed to the Afar plume (Deniel et al., 1994; Pik et al., 1999). Northern Hemisphere Reference Line in (b) and (c) from Hart (1984). Crustal contamination models show effect of fractional crystallisation of DS38 with assimilation of upper crustal (UC; Sr = 69 ppm, Nd = 18.5 ppm, Pb = 48 ppm, $^{87}Sr/^{86}Sr$ = 0.764478, $^{143}Nd/^{144}Nd$ = 0.511398, $^{206}Pb/^{204}Pb$ = 18.598, $^{207}Pb/^{204}Pb$ = 16.026, $^{208}Pb/^{204}Pb$ = 39.746) and lower crustal (UC; Sr = 814 ppm, Nd = 29.94 ppm, Pb = 30 ppm, $^{87}Sr/^{86}Sr$ = 0.709028, $^{143}Nd/^{144}Nd$ = 0.511270, $^{206}Pb/^{204}Pb$ = 16.926, $^{207}Pb/^{204}Pb$ = 15.622, $^{208}Pb/^{204}Pb$ = 37.804) rocks from Davidson and Wilson (1989). Tick marks represent F (fraction of melt remaining) of 0.1%, 0.5%, 1%, 2%, 3%, 4%, 5%.

Figure 8. Primitive mantle normalised La/Yb versus Dy/Yb for lavas from the Siverek phase of the Karacadağ Volcanic Complex. (a) All Siverek phase lavas from Karacadağ Volcanic Complex are compared with melting models using the modal and melting proportions of Thirlwall et al. (1994), distribution coefficients from McKenzie and O'Nions (1991) and initial concentrations and normalisation factors from McDonough and Sun (1995). (b) Siverek data filtered for least crustal contamination as indicated by Ba-enrichment relative to other trace element ratios (e.g. La/Yb, Fig. 6b). The melting model is enriched in middle rare earth elements by

a factor of 1.25 (see text for discussion). Harrat Ash Shaam data from Shaw et al. (2003) and NW Syria data (also filtered for crustal input using Ba-enrichment) from Krienitz et al. (2006). Dashed lines in (b) indicate the likely limits of mixtures produced by melts derived from garnet- and spinel-lherozolite with the tick marks representing gt:sp contributions in the proportions 99:1, 95:5, 90:10 and 80:20. In both panels, melting models show tick marks for the total melt fraction of 0.1%, 0.5%, 1%, 1.5%, 2%, 3%, 4%, 5%, 10%, 15%, 20% and 25%.


N
0
50 Km
MALATYA
ELBİSTAN FAULT
MALATYA FAULT ZONE
EAST ANATOLIAN FAULT ZONE
BİTLİS SUTURE ZONE
SÜRGÜ FAULT
SAVRUN FAULT ZONE
ADIYAMAN FAULT ZONE
DİYARBAKIR
Karacadağ
Ovabağ
Siverek
K.MARAŞ
ADIYAMAN
EAST ANATOLIAN FAULT ZONE
Ceyhan
GAZIANTEP
Tigris River
ŞANLIURFA
Yumurtalık
MEDITERRANEAN SEA
İskenderun
Kilis
SYRIA
DEAD SEA FAULT ZONE
ANTAKYA
Other Miocene and Younger Volcanics
Karacadağ Volcanic Complex
Ovabağ Volcanics (0.29 - 0.53 Ma)
Karacadağ Volcanics (0.91 - 4.50 Ma)
Siverek Volcanics (6.99 - 20.35 Ma)

38°N
39.5°E
40°E
38°N
N
DIYARBAKIR
Pirinçlik
Dağbaşı
Oğlaklı
Dicle
SİVEREK
Karacadağ
Ovabağ
KARACADAĞ
Yücelen
Nohut
Bayırkonak
Şekerli
Bakmaç
Aşağıortaören
Batı
Kazançlı
37.5°N
39.5°E
40°E
5 km
Scale
37.5°N
Midyat Group-
Gaziantep Fm.
(Lower Eocene)
Siverek Volcanics
(Middle-Upper Miocene)
Karacadağ Volcanics
(Pliocene-Lower Pleistocene)
Ovabağ Volcanics
(Upper Pleistocene)
Gölpınar Formation
(Pliocene-Lower Pleistocene)
KARACADAĞ VOLCANIC COMPLEX

Group 1
Group 2
SiO2(wt %)
TiO2(wt %)
Al2O3(wt %)
Fe2O3(wt %)
CaO (wt %)
Na2O (wt %)
K2O (wt %)
P2O5(wt %)
MgO (wt %)
MgO (wt %)

Nb (ppm)
Ba (ppm)
Rb (ppm)
Sr (ppm)
La (ppm)
Zr (ppm)
V (ppm)
Y (ppm)
Group 1
Group 2
MgO (wt %)


Group 1
Primitive Mantle/Rock
Average Primitive Mantle
100
10
1
Cs Rb Ba Th U Nb K La Ce Pb Pr Sr P Nd Zr Sm Eu Ti Dy Y Yb Lu
Group 2
NW Syria, SY-127
(Krienitz et.al., 2006)
Primitive Mantle/Rock
Average Primitive Mantle
100
10
1
Cs Rb Ba Th U Nb K La Ce Pb Pr Sr P Nd Zr Sm Eu Ti Dy Y Yb Lu
3MO103
3MO110
3MO114
Karacadağ Plateau Basalt
(Lustrino et.al, 2010)
Primitive Mantle/Rock
Average Primitive Mantle
1000
100
10
1
Cs Rb Ba Th U Nb K La Ce Pb Pr Sr P Nd Zr Sm Eu Ti Dy Y Yb Lu

NW Syria
Karasu Valley
Other Siverek
Group 2
Group 1
(a)
0,5130
0,5129
0,5128
0,5127
0,5126
0,5125
87Sr / 86Sr
0,703
0,704
0,705
0,706
143Nd / 144Nd
(b)
15,74
15,70
15,66
15,62
15,58
207Pb / 206Pb
18,4
18,6
18,8
19,0
19,2
19,4
206Pb / 204Pb
(c)
39,6
39,4
39,2
39,0
38,8
38,6
38,4
208Pb / 206Pb
18,4
18,6
18,8
19,0
19,2
19,4
206Pb / 204Pb

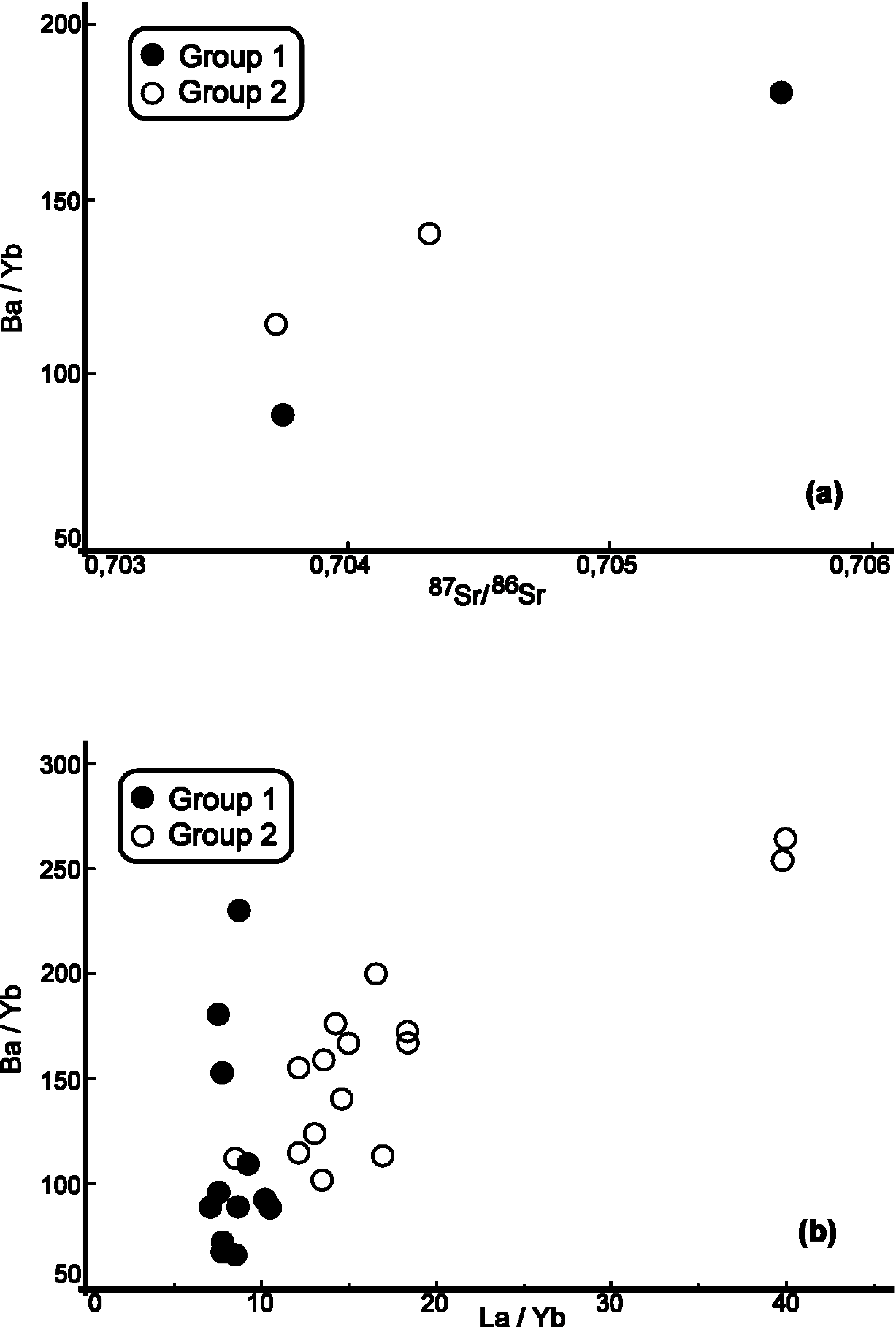

Group 1
Group 2
Ba / Yb
200
150
100
50
0,703
0,704
0,705
0,706
$^{87}Sr/^{86}Sr$
(a)
Group 1
Group 2
Ba / Yb
300
250
200
150
100
50
0
10
20
30
40
La / Yb
(b)

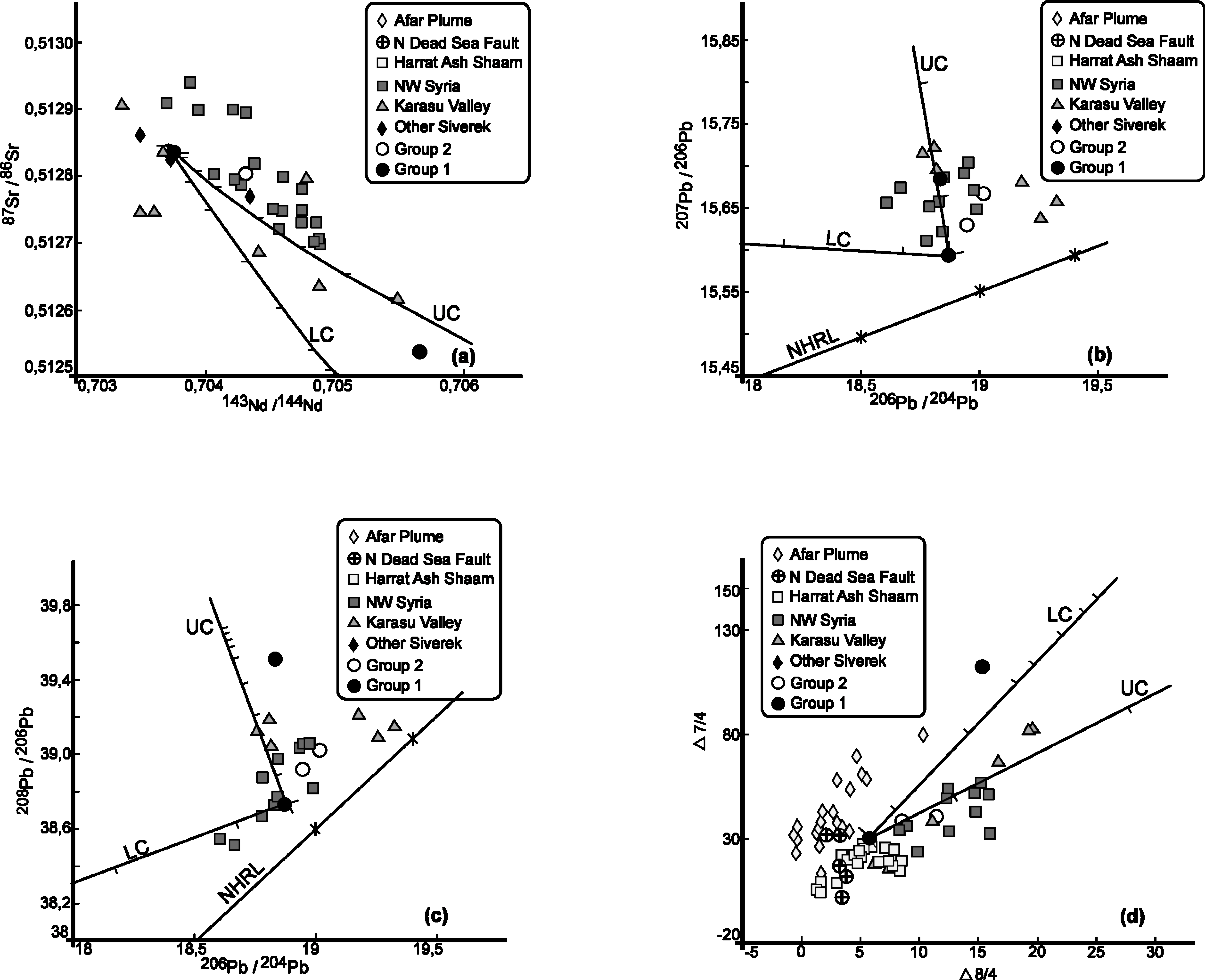

Afar Plume
N Dead Sea Fault
Harrat Ash Shaam
NW Syria
Karasu Valley
Other Siverek
Group 2
Group 1
UC
LC
(a)
87Sr /86Sr
143Nd /144Nd
0,5130
0,5129
0,5128
0,5127
0,5126
0,5125
0,703
0,704
0,705
0,706
NHRL
(b)
207Pb /206Pb
206Pb /204Pb
15,85
15,75
15,65
15,55
15,45
18
18,5
19
19,5
(c)
208Pb /206Pb
39,8
39,4
39,0
38,6
38,2
38
(d)
Δ 7/4
Δ 8/4
150
130
80
30
-20
-5
0
5
10
15
20
25
30

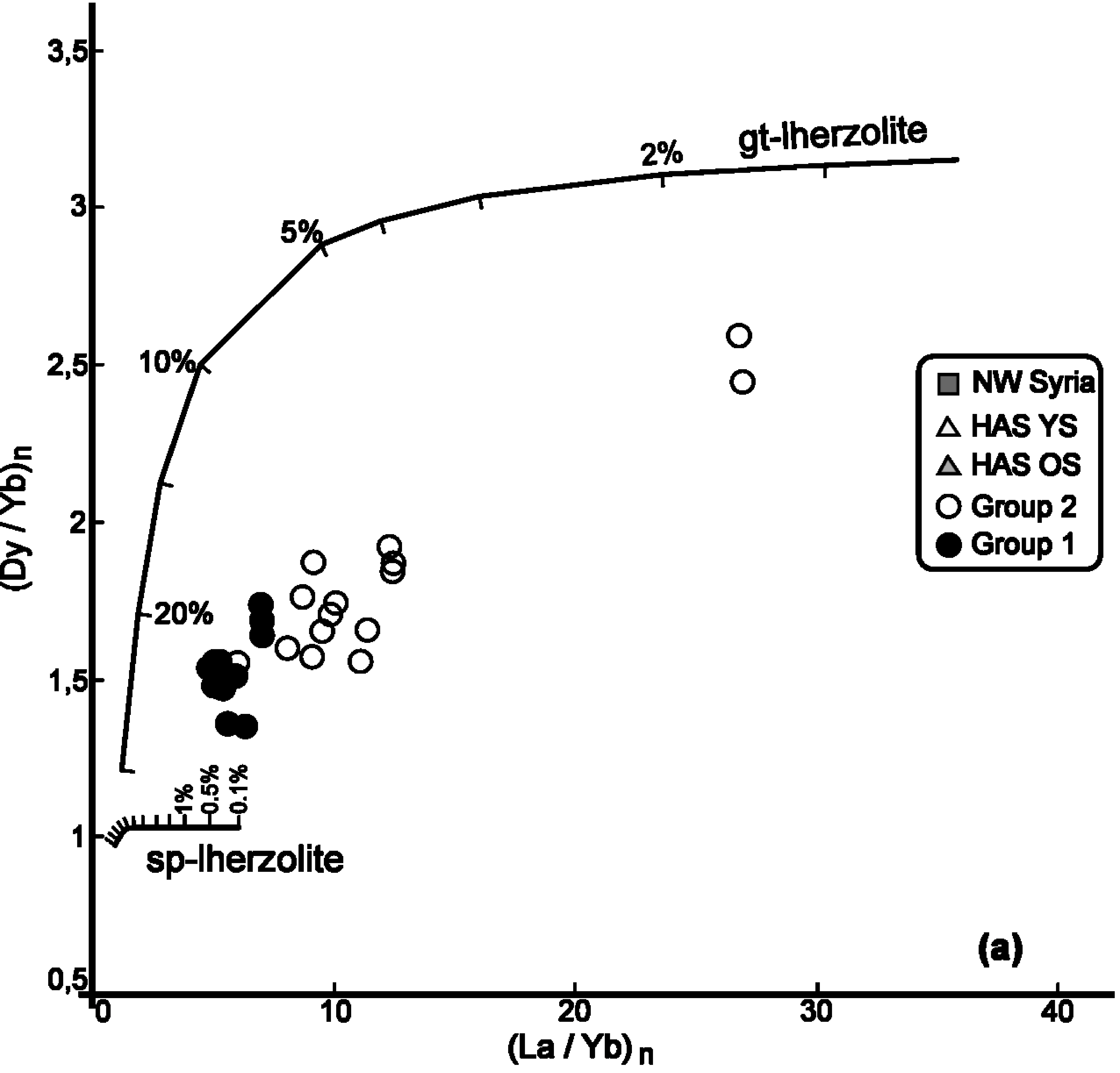

3,5
3
2,5
2
1,5
1
0,5
(Dy / Yb)n
0
10
20
30
40
(La / Yb) n
gt-lherzolite
2%
5%
10%
20%
1%
0.5%
0.1%
sp-lherzolite
NW Syria
HAS YS
HAS OS
Group 2
Group 1
(a)

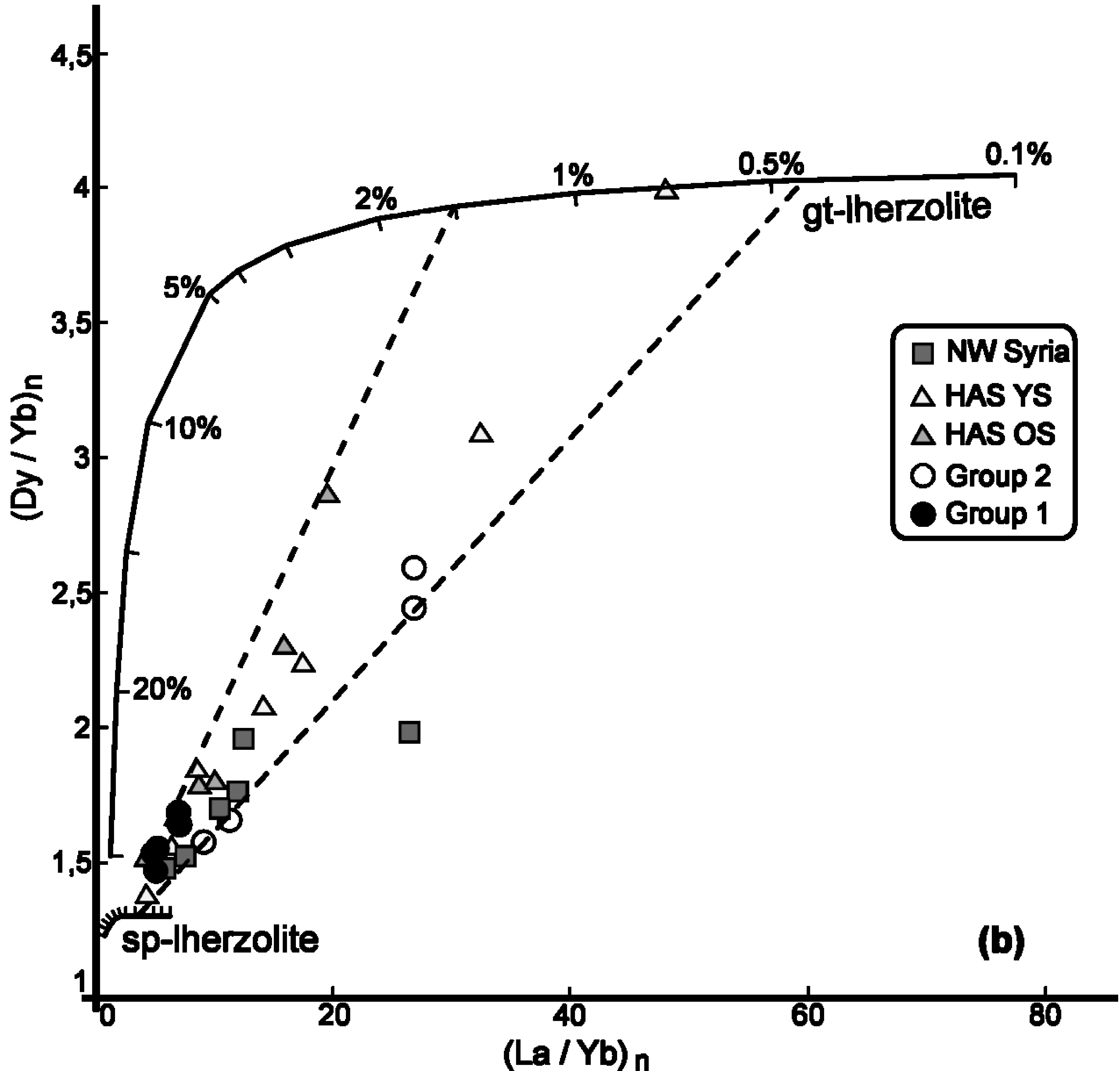

4,5
4
3,5
3
2,5
2
1,5
1
(Dy / Yb)n
0
20
40
60
80
(La / Yb) n
2%
1%
0.5%
0.1%
gt-lherzolite
5%
10%
20%
sp-lherzolite
NW Syria
HAS YS
HAS OS
Group 2
Group 1
(b)